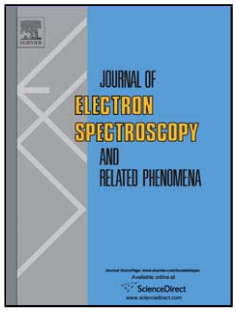

Title: Influence of multiple elastic scattering on the shape of the elastically-scattered electron peak

Authors: V.P. Afanas'ev, M.V. Afanas'ev, A.V. Lubenchenko, A.A. Batrakov, D.S. Efremenko, M. Vos

PII: S0368-2048(10)00005-8
DOI: doi:10.1016/j.elspec.2010.01.002
Reference: ELSPEC 45739

To appear in: *Journal of Electron Spectroscopy and Related Phenomena*

Received date: 20-8-2009
Revised date: 29-11-2009
Accepted date: 11-1-2010

Please cite this article as: V.P. Afanas'ev, M.V. Afanas'ev, A.V. Lubenchenko, A.A. Batrakov, D.S. Efremenko, M. Vos, Influence of multiple elastic scattering on the shape of the elastically-scattered electron peak, *Journal of Electron Spectroscopy and Related Phenomena* (2008), doi:10.1016/j.elspec.2010.01.002

Influence of multiple elastic scattering on the shape of the elastically-scattered electron peak

V.P.Afanas'ev[a], M.V.Afanas'ev[b], A.V.Lubenchenko[a], A.A.Batrakov[a], D.S.Efremenko[a], M.Vos[c]

[a]*Moscow Power Engineering Institute (TU), Krasnokazarmennaya, 14, Moscow 111250, Russia*
[b]*Moscow State Aviation Technological University, Orshanskaya 3, Moscow 121552, Russia*
[c]*Atomic and Molecular Physics Laboratory, Research School of Physical Sciences and Engineering, The Australian National University, Canberra, Australia 0200*

Abstract

The influence of multiple elastic scattering on the shape of the energy distribution of elastically scattered electrons is investigated. The energy of the maximum intensity of the detected electrons differs from the probe electron beam energy due to the elastic energy loss. The experimentally observed spectrum is adequately described by a Gaussian distribution with a maximum at the elastic energy loss value. In this paper the peak-broadening mechanisms due to energy analyzer spread function, probe beam energy distribution and atomic vibration-induced broadening are considered to be independent and of random nature. Analysis of multiple elastic scattering shows some mechanisms leading to the broadening and a shift of the elastic scattering electron energy spectrum from the value defined by single elastic scattering at the certain angle. It is revealed that the magnitude of this shift and the width of energy distrubution is determined by ratio ($l_{\text{in}}/l_{\text{tr}}$), where l_{in} is inelastic mean free pass, l_{tr} is the transport length.

Monte Carlo computation results for elastic energy losses of electrons moving in a solid with stationary atoms are presented as well. The possibility of observing experimentally the elastic peak broadening and shift due to multiple elastic scattering is discussed.

Key words: multiple scattering, electron spectroscopy, elastically reflected electron peak
PACS: 34.80.Bm, 82.80.Yc

1. Introduction

The problem of multiple elastic scattering and its influence on the energy distribution of an elastically scattered electron has been discussed since the end of the 80-ties of the last century [1, 2]. It is closely related to the solution of the classic problem of elastic collisions of an electron (mass — m and energy — E_0) with a motionless nucleus (it's mass is M) on the basis of energy and momentum conservation laws.

There is renewed interest in this problem as experimentally it is now possible to determine the mass of the scattering atom using the recoil effect. In ref.[3] the energy difference of electrons backscattered from Au and C was resolved, making a new method of surface composition analysis feasible. Interpretation in ref.[3] was based on a single scattering model. In this paper we want to investigate if this model is justified.

For single electron scattering over an angle θ_0 (after which the electron moves into an energy analyzer) the energy loss is defined by the kinematic factor $\xi(\theta_0)$[4]:

$$\Delta E = E_0 (2m/M)(1 - \cos\theta_0) = E_0 (1 - \xi(\theta_0)) \quad (1)$$

Alternatively, if deflection over θ_0 is due to n identical scattering events then the energy loss value is given by $\Delta E_n = E_0 n (2m/M)(1 - \cos(\theta_0/n))$. For the case of small angle scattering ($\theta_0/n \to 0$), one can make a series expansion for "cos" and retain the first summand:

$$\Delta E_n = E_0 (m/M)\left(\theta_0^2/n\right) < \Delta E \quad (2)$$

Thus if the total deflection θ_0 (energy analyzer is situated at this angle) is caused by n-times scattering at small angles θ_0/n (we consider here, for simplicity, the case of all scattering events in the same plane), then the energy loss becomes less when the number of scattering events increases. On the other hand if scattering occurs over a larger angle $\theta_0 + \Delta\theta$ at first, and after that over an

Email addresses: AfanasyevVIP@gmail.com (V.P.Afanas'ev), Maarten.Vos@anu.edu.au (M.Vos)

angle $-\Delta\theta$ (again assuming all scattering events in the same plane) then the electron detected at θ_0 will have a larger energy loss than in the single scattering case:

$$\begin{aligned}\Delta E' &= E_0\,(2m/M)\,(1-\cos(\theta_0+\Delta\theta)) + \\ &+ E_0\,(2m/M)\,(1-\cos\Delta\theta) > \\ &> E_0\,(2m/M)\,(1-\cos\theta_0) = \Delta E\end{aligned} \tag{3}$$

It should be noted that the elastic scattering cross-section is strongly forward peaked or, in other words, the probability of small-angle scattering is much larger than the probability of large-angle scattering. Consequently the trajectories leading to smaller energy losses (as in Eq. (2)) are much more probable than the trajectories leading to larger energy losses (see Eq. (3)).

In practice, the measured energy distribution of elastically reflected electrons [5, 6, 7, 8] is a symmetric Gaussian-shaped distribution

$$G_\Sigma(x,\bar{x}) = \frac{1}{\sqrt{2\pi}\sigma_\Sigma}\exp\left(-\frac{(x-\bar{x})^2}{2\sigma_\Sigma^2}\right)$$

with maximum at an energy very close to $E_0 - E_0\xi(\theta_0)$. The width of this Gaussian (σ_Σ) is due to the sum of different contributions: $\sigma_\Sigma = \sqrt{\sigma_D^2+\sigma_A^2+\sigma_B^2}$, where σ_D is broadening due to thermal velocity distribution of the scattering atom (Doppler broadening), σ_A is the energy-analyzer resolution and σ_B is the energy spread in the electron beam. Here we want to investigate if this interpretation is correct, or that the effect of the multiple elastic collisions on the energy distribution should be considered as well in the interpretation of σ_Σ.

In this paper we consider that the atoms in a solid are motionless — i.e. we neglect the Doppler broadening ($\sigma_D = 0$). In our model the broadening due to the electron gun energy spread and the finite energy-analyzer resolution are also not taken into account ($\sigma_B = 0$), ($\sigma_A = 0$). The purpose of this model is to determine the influence of multiple elastic collisions on the elastically-scattered electron energy distribution. Two analytical models for multiple elastic scattering that describe the energy shift and broadening of the elastic peak will be considered.

The first model corresponds to the situation where an electron, after strong scattering over the angle θ_0, undergoes multiple small-angle scatterings, but the average directional change due to these small-angle scattering events averages out to 0. Along its trajectory elastic energy losses occur that are proportional to the path length. *The second model* corresponds to the case where strong scattering occurs over an angle $\theta_0 \pm \theta$, but after that, and before coming into the energy analyzer, the electron scatters again and the propagation direction changes by $\mp\theta$. Both cases are discussed for the homogeneous medium without boundaries (Goudsmit-Saunderson approximation [9]).

The boundary problem will be solved using Monte-Carlo simulations describing multiple binary electron collisions in a medium of randomly-located motionless atoms.

2. Multiple elastic energy losses

Let's consider an electron flux propagating in a solid over a distance dx. As a consequence of momentum and energy conservation the energy loss for scattering over θ is defined by Eq. (1). The probability of scattering over an angle θ is defined by the differential elastic scattering cross-section $\omega_e(\theta)$. The probability of elastic scattering with a sample atom over the interval dx is proportional to ndx, where n is the concentration of scatterers (atoms). Integrating Eq. (1) over θ we get the following:

$$\begin{aligned}dE_{el} = ndxE_0\int_0^\pi \frac{2m}{M}\,(1-\cos\Delta\theta)\,\omega_e(\Delta\theta)\,d\Delta\theta = \\ = ndxE_0\,(2m/M)\,\sigma_{tr}\end{aligned} \tag{4}$$

Here σ_{tr} is transport cross-section. From Eq. (4) the mean energy loss per unit length (i.e. "elastic stopping power") can be determined:

$$dE_{el}/dx = nE_0\,(2m/M)\,\sigma_{tr} = (2m/M)\,(E_0/l_{tr}) \tag{5}$$

The energy of an electron slowing down can only decrease. This leads to an asymmetry in the energy distribution of the elastically-reflected electrons.

The elastic transmission function $T_e^{GS}(x,\Delta\theta)$ is of great importance. It defines the probability that an electron, passing a length x, changes its direction of movement by $\Delta\theta$. An equivalent problem was solved by Goudsmit and Saunderson [9] before. However a somewhat different solution that allows us to picture more clearly the mechanism of energy losses due to multiple elastic scattering will be given. Note that the expression

$$\exp(-\sigma_e nx)\,\frac{(\sigma_e nx)^j}{j!} \tag{6}$$

is a Poisson distribution defining the probability of j independent events (j scatterings in our case) on the interval x.

Let's write $T_e^{GS}(x, \Delta\theta)$ as the sum of particles that have scattered 0,1,2... times

$$T_e^{GS}(x,\Delta\theta) = \exp(-\sigma_e n x)\left[\delta(\Delta\theta) + \frac{nx}{1!}\omega_e(\Delta\theta) + \right. \\ \left. + \sum_{j=2,3...} \frac{(nx)^j}{j!}\overline{\omega_e(\Delta\theta)}^j\right], \quad (7)$$

with

$$\overline{\omega_e(\Delta\theta)}^j = \int_{4\pi} \overline{\omega_e(\Delta\theta - \Delta\theta')}^{j-1}\omega_e(\Delta\theta')\, d\varphi' d\cos\Delta\theta',$$

δ is the Dirac delta function, $\omega_e(\Delta\theta')$ is the differential cross-section of electron elastic scattering by atom [4], σ_e is the total elastic scattering cross-section, $\int_{4\pi} d\varphi' d\cos\Delta\theta' = \int_0^{2\pi} d\varphi' \int_{-1}^{1} d\cos\Delta\theta'$. Now make a Legendre series expansion of the differential elastic cross-section:

$$\omega_e(\Delta\theta) = \sum_{l=0}^{\infty} \frac{2l+1}{4\pi}\omega_l P_l(\cos\Delta\theta) \quad (8)$$

The expansion coefficients, as it follows from Eq. (8), are defined by:

$$\omega_l = \int_{4\pi} \omega_e(\Delta\theta) P_l(\cos\Delta\theta)\, d\cos\Delta\theta d\varphi \quad (9)$$

The property of completeness of the Legendre Polynomials allows us to write:

$$\delta(\Delta\theta) = \sum_{l=0}^{\infty} \frac{2l+1}{4\pi} P_l(\cos\Delta\theta) \quad (10)$$

Substituting Eqs. (8) –(10) into Eq. (7) and calculating the integral (using the orthogonality of Legendre polymomials) we obtain:

$$T_e^{GS}(x,\Delta\theta) = \exp(-\sigma_e n x)\times \\ \times \sum_{l=0}^{\infty} \frac{2l+1}{4\pi} P_l(\cos\Delta\theta)\left[1 + \sum_{j=1,2,...} \frac{(nx)^j}{j!}\omega_l^j\right] \quad (11)$$

From Eq. (11) one can derive the Goudsmit and Saunderson solution in its classical form:

$$T_e^{GS}(x,\Delta\theta) = \\ = \exp(-\sigma_e n x) \sum_{l=0}^{\infty} \frac{2l+1}{4\pi} P_l(\cos\Delta\theta)\exp(\omega_l n x) \quad (12)$$

It is obvious that $\sigma_e = \omega_0$. Thus Eq. (12) has another form:

$$T_e^{GS}(x,\Delta\theta) = \\ = \sum_{l=0}^{\infty} \frac{2l+1}{4\pi} P_l(\cos\Delta\theta)\exp[-(\omega_0 - \omega_l) n x] \quad (13)$$

Now consider the coefficients in the exponent of Eq. (13). Using Eq. (9) we get:

$$\omega_0 - \omega_l = \int_{4\pi} d\cos\Delta\theta d\varphi \omega_e(\Delta\theta)(1 - P_l(\cos\Delta\theta)) \quad (14)$$

From Eq. (14) we can write:

$$\omega_0 - \omega_1 = \int_{4\pi} d\cos\Delta\theta d\varphi \omega_e(\Delta\theta)(1 - \cos\Delta\theta) = \sigma_{tr} \quad (15)$$

3. The influence of elastically scattered electrons entering the analyzer after multiple scatterings on the energy spectrum form

Let us again consider an infinite medium. The z-axis is chosen in the direction of the energy analyzer. The mono-energetic unidirectional electron beam makes an angle θ with the z-axis. The following classes of trajectories contribute to the spectra:

A) trajectories that were strongly scattered over an angle θ and then coming into the entrance slit without further collisions;

B) trajectories that have scattered over an angle $\theta + \Delta\theta$ ($\theta + \Delta\theta$ is an angle to axis z, but azimuth angle can be unspecified), but are subsequently scattered in such a way that they travel along the z-axis.

We are interested in two questions:

1. What is the value and sign ("plus" or "minus") of the energy shift in case B compared to case A?

2. What is the contribution of these processes to the energy distribution of elastically scattered electrons?

These questions arise because the trajectories mentioned under B reach the energy analyzer after elastically scattering two, three or more times. The energy loss associated with the scattering at the angle $\theta + \Delta\theta$ is described by the following expression:

$$\Delta E' = E_0(2m/M)(1 - \cos(\theta + \Delta\theta)) = \\ = E_0(2m/M)(1 - \cos\theta + \cos\theta - \cos(\theta + \Delta\theta)) = \\ = \Delta E + E_0(2m/M)(\cos\theta - \cos(\theta + \Delta\theta)) = \\ = \Delta E + \Delta E_1 \quad (16)$$

with

$$\cos(\theta + \Delta\theta) = \cos\theta\cos\Delta\theta - \sin\theta\sin\Delta\theta\cos\varphi \quad (17)$$

Now let us find the corresponding energy shift:

$$\overline{\Delta E_1} = \int_{4\pi} d\cos\Delta\theta d\varphi T_e^{GS}(x,\Delta\theta)\Delta E_1 \quad (18)$$

Eq. (18) can be evaluated either using Eq. (6) or Eq. (13). Usage of Eq. (6) makes Eq. (16) clearly evident:

$$\overline{\Delta E_1} = \int_{4\pi} d\cos\Delta\theta d\varphi \exp\left(-\sigma_e n x\right) \times$$
$$\times \left[\delta\left(\Delta\theta\right) + \frac{nx}{1!}\omega_e\left(\Delta\theta\right) + \sum_{j=2,3\ldots} \frac{(nx)^j}{j!}\overline{\omega_e\left(\Delta\theta\right)}^j\right] \times$$
$$\times E_0\left(2m/M\right)\left(\cos\theta - \cos\theta\cos\Delta\theta + \sin\theta\sin\Delta\theta\cos\varphi\right) \tag{19}$$

But numeric calculations (this will be obvious later) can be done more easily using Eq. (13). After integration of Eq. (19) over φ and taking into account

$$\int_0^{2\pi} d\varphi\cos\varphi = 0 \tag{20}$$

we get:

$$\overline{\Delta E_1} = 2\pi\int_{-1}^{+1} d\cos\Delta\theta\cdot\exp\left(-\sigma_e n x\right) \times$$
$$\times \left[\delta\left(\Delta\theta\right) + \frac{nx}{1!}\omega_e\left(\Delta\theta\right) + \sum_{j=2,3\ldots} \frac{(nx)^j}{j!}\overline{\omega_e\left(\Delta\theta\right)}^j\right] \times \tag{21}$$
$$\times E_0\left(2m/M\right)\left(\cos\theta - \cos\theta\cos\Delta\theta\right)$$

Let us now consider Eq. (21) in more detail. The first term in the square brackets integrates out to 0 as: $\int_{-1}^{+1} d\cos\Delta\theta\left(\cos\theta - \cos\theta\cos\Delta\theta\right)\delta\left(\Delta\theta\right) = 0$. This term describes the fact that the particles after a strong scattering at the angle $\theta \pm \Delta\theta$ can come into energy analyzer only because of additional elastic scatterings. The second term in the square brackets of Eq. (21) describes the particles, that having been scattered over an angle $\theta \pm \Delta\theta$ and enter the energy analyzer after additional single elastic scattering over an angle $\mp\Delta\theta$.

The integration over the azimuth angle in Eq. (19) leads to smoothing of positive (see Eq. (2)) or negative (see Eq. (1)) additives to the energy ΔE. The smoothing is the consequence of our consideration of scattering process in an infinite medium. Boundary conditions influence the integration limits over the azimuth angle in Eq. (19) and can lead to the domination of processes resulting in a reduction of the energy losses ΔE (see Eq. (1)) (this will be shown further using Monte-Carlo simulation). Boundary conditions have also a strong influence of the processes that lead to an increase of the energy loss ΔE (see Eq. (2)).

The third term in square brackets of Eq. (21) describes the particles that having been scattered at the angle $\theta \pm \Delta\theta$ and enter the energy analyzer after scattering $j = 2, 3\ldots$ times resulting in a total directional change of $\mp\Delta\theta$ etc.

Let us execute the certain calculations replacing the expression in the square brackets of Eq. (21) on the Eq. (13) in Legendre series form:

$$\overline{\Delta E_1} = 2\pi\int_{-1}^{+1} d\cos\Delta\theta\times$$
$$\times\left\{\sum_{l=0}^{\infty}\frac{2l+1}{4\pi}P_l\left(\cos\Delta\theta\right)\exp\left[-\left(\omega_0 - \omega_l\right)nx\right]\right\}\times$$
$$\times E_0\left(2m/M\right)\left(\cos\theta - \cos\theta\cdot P_1\left(\cos\Delta\theta\right)\right) \tag{22}$$

In the last line of Eq. (22) we used: $P_1\left(\cos\Delta\theta\right) \equiv \cos\Delta\theta$. Integrating in Eq. (22) is easily done. Using the orthogonality property of Legendre polynomials we obtain for the shift in the peak position:

$$\overline{\Delta E_1} = E_0\left(2m/M\right)\cos\theta\left(1 - \exp\left[-\left(\omega_0 - \omega_1\right)nx\right]\right) \tag{23}$$

Or by taking into account Eq. (15) and that transport length $l_{tr} = 1/\left(\sigma_{tr} n\right)$ we get:

$$\overline{\Delta E_1} = E_0\left(2m/M\right)\cos\theta\left(1 - \exp\left(-x/l_{tr}\right)\right) \tag{24}$$

If $x \ll l_{tr}$ then, by using only the first two terms of the series expansion of the exponent in Eq. (24), we can approximate this result by:

$$\overline{\Delta E_1} = E_0\left(2m/M\right)\cdot\cos\theta\cdot\frac{x}{l_{tr}} = dE_{el}/dx\cdot\cos\theta\cdot x \tag{25}$$

Now we continue with the estimation of the root-mean-square deviation (i.e. the broadening of the peak):

$$\sqrt{\overline{\Delta E_1^2}} = \sqrt{\int_{4\pi} d\cos\Delta\theta d\varphi T_e^{GS}\left(x,\Delta\theta\right)\Delta E_1^2} \tag{26}$$

Squaring $\left(\cos\theta - \cos\theta\cos\Delta\theta + \sin\theta\sin\Delta\theta\cos\varphi\right)$ and integrating over $d\varphi$, we obtain:

$$\int_0^{2\pi} d\varphi(\cos\theta - \cos\theta\cos\Delta\theta + \sin\theta\sin\Delta\theta\cos\varphi)^2 =$$
$$= \left(\cos^2\theta + \frac{1}{2}\sin^2\theta\right) -$$
$$- 2\cos^2\theta\cos\Delta\theta + \left(\cos^2\theta - \frac{1}{2}\sin^2\theta\right)\cos^2\Delta\theta$$

Here we have used the equalities: $\int_0^{2\pi} d\varphi \cos\varphi = 0$, $\int_0^{2\pi} d\varphi \cos^2\varphi = 1/2$. Since $\cos\Delta\theta = P_1(\cos\Delta\theta)$, $\cos^2\Delta\theta = (2P_2(\cos\Delta\theta)+1)/3$, the root-mean-square deviation $\sqrt{\overline{\Delta E_1^2}}$ can be written in the following form:

$$\sqrt{\overline{\Delta E_1^2}} = E_0(2m/M)\times \times\left\{\int_{-1}^{1} d\cos\Delta\theta \cdot T_e^{GS}(x,\Delta\theta)\times \times\left[\frac{1}{3}\left(1+3\cos^2\theta\right)-2\left(\cos^2\theta\right)P_1(\Delta\theta)- -\frac{1}{3}\left(1-3\cos^2\theta\right)P_2(\Delta\theta)\right]\right\}^{1/2} \quad (27)$$

After integrating of Eq. (27) we get:

$$\sqrt{\overline{\Delta E_1^2}} = E_0(2m/M)\times \times\left\{\frac{1}{3}\left(1+3\cos^2\theta\right)-2\left(\cos^2\theta\right)\exp\left(-\frac{x}{l_{tr}}\right)- -\frac{1}{3}\left(1-3\cos^2\theta\right)\exp\left(-\frac{3x}{l_{tr}}\right)\right\}^{1/2} \quad (28)$$

If $x \ll l_{tr}$ then we can make a series expansion of the exponent in Eq. (28) and by retaining the first two terms we get:

$$\sqrt{\overline{\Delta E_1^2}} = E_0(2m/M)|\sin\theta|\sqrt{\frac{x}{l_{tr}}} \quad (29)$$

The value of x for the considered problem is of the order of the inelastic mean free path: $x \simeq l_{in}$. As for $x \gg l_{in}$ the probability that such a trajectory contributes to the elastic peak in very small. The most important result of the current paragraph is the fact that a factor

$$\varepsilon_{SHIFT} = l_{in}\cdot dE_{el}/dx = E_0(2m/M)\frac{l_{in}}{l_{tr}} \quad (30)$$

describes the elastic peak energy shift due to the processes of continuous elastic energy losses (see Eq. (5)) as well as the processes of multiple elastic scattering. The factor

$$\varepsilon_{WIDTH} = \sqrt{\overline{\varepsilon_{el}^2 l_{in}}} = E_0(2m/M)\sqrt{\frac{l_{in}}{l_{tr}}} \quad (31)$$

describes the broadening of the elastic peak energy distribution.

The effect of multiple scattering depends thus on the values of l_{in} and l_{tr} . These quantities are plotted in fig. 1 for C and Au. The quantities ε_{SHIFT} and ε_{WIDTH} are plotted on Fig. 2 as a function of energy. l_{in} was calculated by TPP-2M formula [12]. Values of l_{tr} were taken from [13]. The weak dependence of the parameter (30) and (31) on energy and their small influences on the energy distribution are evident. This parameter describes the distribution of multiple elastic scattering energy losses. It is important to note that the energy broadening is larger than the shift by an order of magnitude. Note that the curves of ε_{SHIFT} of C and Au crosses. This is a consequence of the fact that l_{tr} increases faster with energy for C than for Au.

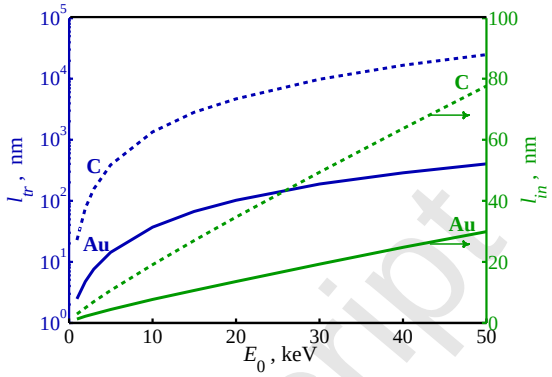

Fig. 1: The transport mean free path l_{tr} (log vertical scale) and the inelastic mean free path l_{in} (linear vertical scale) for C and Au for the energies of interest.

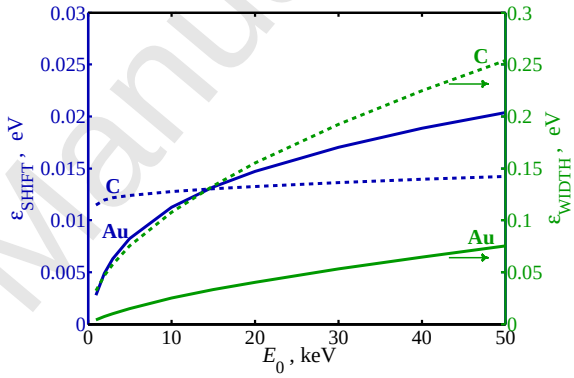

Fig. 2: The dependence of peak position shift (see Eq. (30)) due to multiple scattering and the dependence of the peak width (see Eq. (31)) due to multiple scattering on the incoming energy.

4. Monte-Carlo (MC) simulation of multiple elastic scattering in a medium with stationary atoms

Monte-Carlo simulations of multiple elastic scatterings are carried out on the basis of the binary collision

approximation [10, 11]. The cross-sections of inelastic and elastic scattering are chosen in accordance with Ref. [12, 13]. After an electron has scattered inelastically, we are not interested in it any more (the electron is then considered "dead", as it can not contribute anymore to the elastic peak), and hence the simulation of such a trajectory is aborted. The probability of an electron "surviving" each scattering event is defined by the albedo for single scattering $\lambda = \sigma_{\text{el}}/(\sigma_{\text{el}} + \sigma_{\text{in}})$.

About $N = 3 \times 10^9$ trajectories for each case are simulated. The particle's trajectory is simulated by a straight-forward Monte-Carlo method based on the mean free path (the mean distance between two junction points) and the randomly distribution of the scattering events (elastic or inelastic) in the certain point. After the scattering event the particle propagates along a new direction and with a reduced energy until the next collision occurs.

5. Results and discussion

In the simulations the incoming beam direction, surface normal and outgoing electrons (that are detected by the analyzer) are chosen in a single plane. The angle of incidence equals 67.5°. In the first case the scattering angle is 45° and in the second case it is 180°.

$R(\Omega_0, \Omega, \Delta)$ denotes spectrum of elastically scattered particles (Ω_0 and Ω are incident and outgoing solid angles respectively).

The area under elastic peak can be estimated as $r(\Omega_0, \Omega) = \int_0^{E_0} R(\Omega_0, \Omega, \Delta)\, d\Delta$.

A spectrum obtained by the Monte Carlo simulation is shown in Fig. 3 and consists of a superposition of a sharp peak (due to electrons scattered in a single collision over an angle θ_0) and a broad "dome" (due to electrons coming into the analyzer after multiple elastically scattering events). The normalization of the spectra is implemented in accordance with the exact solution of the angular distribution problem for particles reflected by multilayer slabs with defined elastic cross-section and albedo for each slab [14].

The results of the exact calculation of the reflection function for the spatial angle of 10^{-5} sr for Au and C samples for two different scattering geometries are plotted on the Fig. 4.

The contribution of single scattered particles to the total signal is an order of magnitude smaller than that of multiple scattered ones.

The energy spectrum shown in Fig. 3 illustrates the dominating influence of multiple elastic scattering. But here the Doppler broadening due to the thermal motion,

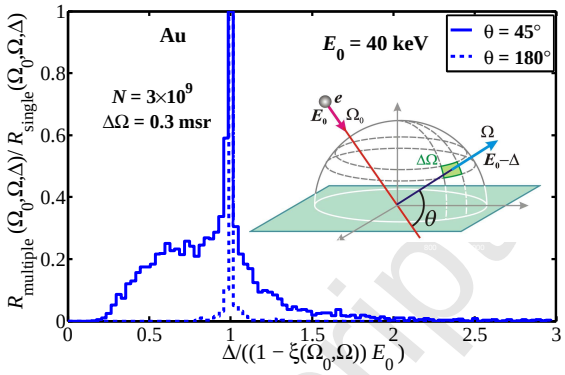

Fig. 3: The form of energy spectrum of elastically reflected electrons obtained by Monte-Carlo calculation for incident angle 67.5°, the scattering angles are 45° and 180°

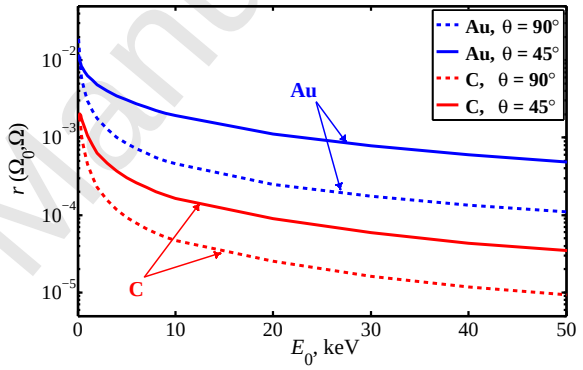

Fig. 4: Exact solution for reflection electron beam intensity in the cases of two geometries for C and Au samples. $r(\Omega_0, \Omega)$ corresponds to the fraction of the incoming beam that is reflected without inelastic energy loss, into the analyzer with Ω_0, Ω — incident and outgoing angles respectively and without azimuth rotation ($\Delta\varphi = 0$).

the finite energy resolution of the analyzer and the energy distribution of the probe beam are not taken into account.

In the Fig. 5 we investigate if the influence of multiple scattering can be seen, when energy broadening is taken into accout. The following curves are shown: solid and non-monotonic curve is Monte-Carlo simulation result $R_{\text{MC}}(\Omega, \Omega_0, \varepsilon)$; solid and monotonic curves are the convolutions of previous curve with Gaussian function (subscript"br" means *broadened*):

$$R_{\text{br}}(\Omega, \Omega_0, \Delta) = \int_0^{E_0} R_{\text{MC}}(\Omega, \Omega_0, \varepsilon)\, G_\Sigma(x, \varepsilon)\, d\varepsilon; \quad (32)$$

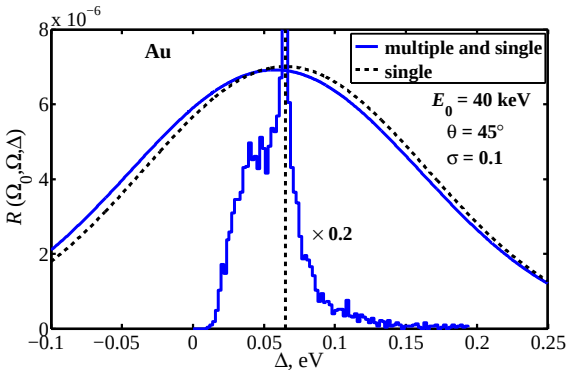

Fig. 5: Spectrum of electrons elastically reflected from Au, E_0=40 keV, the scattering is in the plane that is perpendicular to the sample one. Incident angle — 67.5°, reflection angle — 67.5°, scattering angle — θ =45°. $R_{\rm br}(\Omega,\Omega_0,\Delta)$ — solid smooth line; $R(\Omega,\Omega_0,\Delta)$ — dotted smooth line; $R_{\rm MC}(\Omega,\Omega_0,\Delta)$ — histogram; the vertical dotted smooth line describes the function $\delta[\Delta-(1-\xi(\theta))E_0]$ corresponding to the simple electron scattering at the angle θ from motionless atom of a sample, $\xi(\theta)$ — the kinematic factor (see Eq. (1)).

dotted line is a such function:

$$R(\Omega,\Omega_0,\Delta) = \\ = \int_0^{E_0} \delta(\varepsilon-(1-\xi(\theta))E_0)\,G_\Sigma(x,\varepsilon)\,d\varepsilon = \\ = \frac{1}{\sqrt{2\pi}\sigma_\Sigma}\exp\left(-\frac{(\Delta-(1-\xi(\theta))E_0)^2}{2\sigma_\Sigma^2}\right) \qquad (33)$$

calculated without taking into account energy losses for multiple elastic scattering in the simple scattering approximation (ε is a variable of integration). The Gaussian function with σ_Σ in Eqs. (32, 33) describes the total broadening of signal due to Doppler effect, finite energy resolution of the analyzer, and energy spread of the probe beam.

Fig. 5 shows that if $\sigma_\Sigma \geq 0.1$ eV the curves described by $R_{\rm br}(\Omega,\Omega_0,\Delta)$ and $R(\Omega,\Omega_0,\Delta)$ practically coincide. The shift of energy distribution maximum $\Delta E \approx 0.03$ eV is clearly observed. This is in good agreement with the value of the shift parameter (30) $E_0\,(2m/M)\cdot l_{\rm in}/l_{\rm tr}$, (0.019 eV — see Fig. 2) as it was obtained by the analytical theory.

The dominant part of the multiple scattered particle energy spectrum are the electrons with energy losses less than ΔE value as calculated from Eq. (1). This means that the contribution in the spectrum of electrons coming into the energy analyzer due to multiple small angle scatterings (with energy losses defined by Eq. (2)) appreciably exceeds the contribution of electrons with even one elastic scattering at the angle more than θ_0

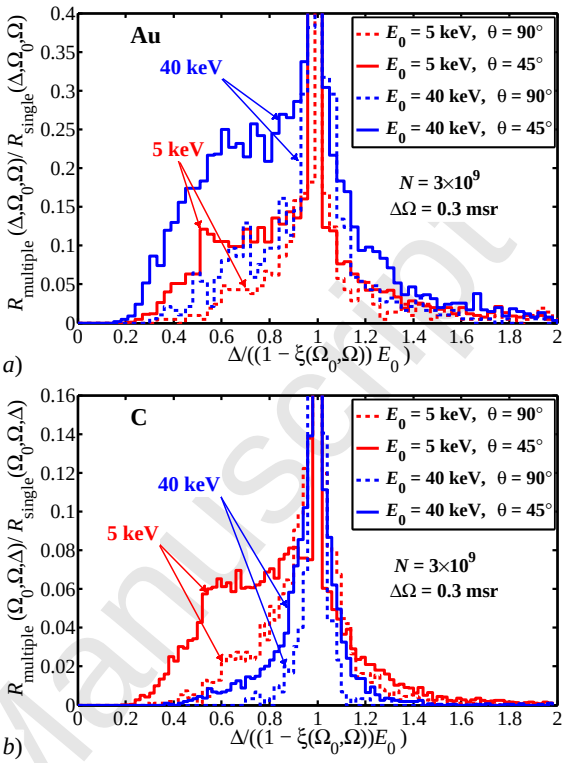

Fig. 6: The normalized spectra (obtained by Monte Carlo simulations) of electrons elastically reflected from *a*) — Au and *b*) — C; the energy scale is in units of the single-scattering recoil energy (Eq. 1)

(with energy losses defined by Eq. (3)). This is a consequence of the fact that the cross-section is peaked in the forward direction — i.e. the probability of a small-angle scattering event is much larger than the probability of large-angle scattering event.

Fig. 6 illustrates the influence of energy and scattering geometry on the energy distribution of elastically scattered electrons. These results can be compared with the shift and width as defined values defined by eq. (30) and eq.(31). When the energy increases and the geometry is left unchanged then the root-mean-square deviation increases as well (see Fig. 2).

Also an adequate agreement between the analytical calculation (see Fig. 2) and the Monte Carlo simulation (see Fig. 3) is observed. The calculated broadening of spectra (see Eq. (29)) is in a good agreement with Monte Carlo simulation.

We can see on Fig. 6 that all features of the scattering on Au are the same ones for the scattering on C. The larger broadening of C spectra (larger than the broadening of the Au spectra) is in accordance with analytical theory. It is a consequence from Monte Carlo simulation that for C the contribution of singly-scattered electrons

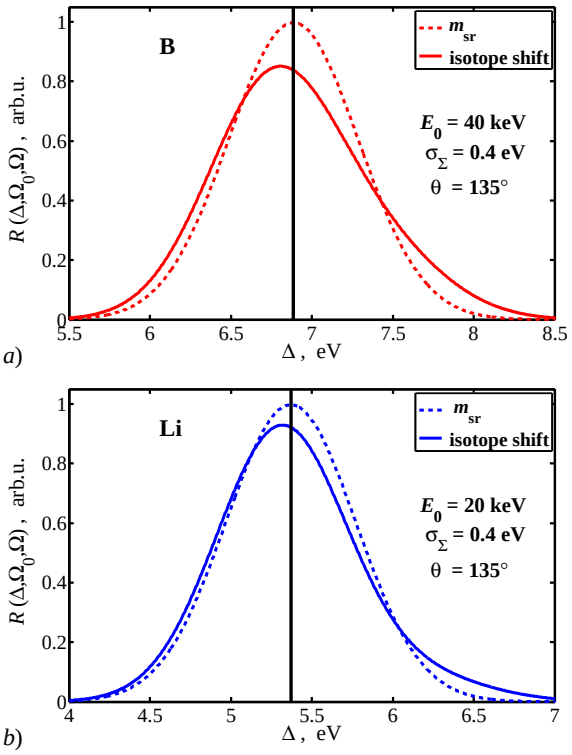

Fig. 7: Peak shape of electrons elastically reflected from *a*) — B and *b*) — Li samples for incoming energies as indicated. The solid line — the spectrum of electrons elastically reflected from one isotope sample with average mass, the dotted line — the calculation considering different masses and abundance on the Earth [15].

and multiple scattered electrons are of the same order of magnitude. The case of 40 keV electron scattering from carbon was not simulated as, due to the smallness of the scattering cross sections at these energies, a Monte Carlo simulation is not practical under these conditions. Under these conditions the Doppler broadening of the C peak is very significant making it again unlikely that effects due to multiple scattering are resolved in the experiment.

Finally we study one more possible cause of an asymmetry of homogeneous reflected electron peak. It deals with different concentration of isotopes [15] in materials. In Fig. 7 the elastically reflected electron peaks calculated with provision for different isotope abundance are shown. The calculations are done for B, Li, Si and Mo. Unlike the effect of multiple scattering which requires an energy resolution of $\sigma_\Sigma = \sqrt{{\sigma_D}^2 + {\sigma_A}^2 + {\sigma_B}^2} \simeq 0.1$ eV to observe it, the isotope broadening effect for B and Li can be observed at $E_0 = 20 - 40$ keV with an experimental resolution of 0.4 eV.

6. Conclusion

These investigations have shown that under actual experimental conditions the interpretation of the elastic peak spectra in terms of a single scattering model is justified. Although multiple scattering occurs frequently, the effect of multiple scattering on the energy distribution and peak position is usually very small, considerably less than the experimental resolution. Thus interpretation of the elastic peak in terms of sample composition and a single scattering model is possible and makes this method a promising candidate for the composition studies of intermediate thicknesses.

We have investigated the influence of multiple elastic scattering on the elastically scattered electron peak at energy 5-40 keV. In papers [16, 17] the analysis is implemented for energy 1–2 keV by Monte-Carlo simulation. Significant influence on elastic peak shape have not been found. The similar conclusions about weak influence of multiple scattering on the shape of elastically scattered electron peak for energy 500–3000 eV are in paper [18].

References

[1] N.E. Erickson , C.J. Powell. Phys. Rev. B 40(1989)7284.
[2] D. Laser, P. Seah Phys. Rev. B 47(1993)9836.
[3] M.J. Went, M. Vos, R. Elliman, Journal of Electron Spectroscopy and Related Phenomena 156 (2007) 387
[4] W-K.Chu, J.W.Mayer, M.A.Nicolet, Backscattering Spectrometry, Academic Press, New York, 1978.
[5] M. Vos, Ultramicroscopy 92(2002)143.
[6] M. Vos, C.A.. Chatzidimitriou-Dreismann, T. Abdul-Redah. and J. Mayers. , Nucl. Instum. and Meth. B 227(2005)233.
[7] M.R. Went, M. Vos, Surface Science 600 (2006) 2070.
[8] M. Vos, G.P. Cornish, E. Weigold, Rev. Sci. Instrum. 71(2000)3831.
[9] S. Goudsmit, J.L. Saunderson, Phys. Rev. 57(1940)24.
[10] M. Dapor, Phys. Rev. B 46(1992)618
[11] I.M. Sobol, The Monte Carlo Method, MIR, Moscow, 1975.
[12] S. Tanuma, C.J. Powell, D.R. Penn, Surf. Interf. Anal. 20(1993)77.
[13] F. Salvat, A.. Jablonski, C.J. Powel, Comput. Phys. Commun. 165(2005)157.
[14] V.P. Budak, S.V. Korkin, J. of Quant. Spectrosc. and Rad. Trans. 109(2008)220.
[15] Tables of isotopes/Ed. By C. M.Lederer, V.S. Shirley, 7th ed., Willy, New York, 1978.
[16] F. Yubero, V.J. Rico, J.P. Espinos, J. Cotrino and A.R. Gonzalez-Elipe, Appl. Phys. Lett. 87(2005)084101.
[17] F. Yubero and K. Tokesi, Appl. Phys. Lett. 95(2009)084101.
[18] W.S.M. Werner, C. Tomastik, T. Cabela, G. Richter, H. Stori, J. Electron Spectrosc. Relat. Phenom. 113(2001)127.